Theoretical Study of the Solvation of Fluorine and Chlorine Anions by Water

Daniel D. Kemp and Mark S. Gordon*

Department of Chemistry, Iowa State University, Ames, Iowa 50011

Received: March 8, 2005

The solvation of fluoride and chloride anions (F^- and Cl^-, respectively) by water has been studied using effective fragment potentials (EFPs) for the water molecules and ab initio quantum mechanics for the anions. In particular, the number of water molecules required to fully surround each anion has been investigated. Monte Carlo calculations have been used in an attempt to find the solvated system $X^-(H_2O)_n$ (X = F, Cl) with the lowest energy for each value of *n*. It is predicted that 18 water molecules are required to form a complete solvation shell around a Cl^- anion, where "complete solvation" is interpreted as an ion that is completely surrounded by solvent molecules. Although fewer water molecules may fully solvate the Cl^- anion, such structures are higher in energy than partially solvated molecules, up to $n \geq 18$. Calculations on the F^- anion suggest that 15 water molecules are required for a complete solvation shell. The EFP predictions are in good agreement with the relative energies predicted by ab initio energy calculations at the EFP geometries.

I. Introduction

Solvation effects have an important role in many different areas of chemistry. Spectroscopy, reaction mechanisms, and kinetics are examples of phenomena that are affected by the presence or absence of a solvent. In this study, the effective fragment potential (EFP) method[1,2] is employed to investigate the solvation of fluoride and chloride anions (F^- and Cl^-, respectively). Water-solvated Cl^- and F^- anions have been the subject of many other theoretical studies[3−48] and several relevant experimental studies[49,50] have been performed on the chloride ion. Smaller water clusters, usually involving <10 water molecules, are most common, because of computational limitations. When applied to a halide anion X^-, the focus of many microsolvation studies is to determine how many water molecules are required to observe a transition from a surface to an interior state. A surface state is defined as the X^- anion resting "on top" of a cluster of water molecules, while an interior state is defined as a structure in which the X^- anion is "inside" a water cluster cage.

The primary focus of this study is to analyze the transition from surface to completely solvated anions in $X^-(H_2O)_n$ (X = F, Cl) as *n* increases. Also of interest is the value of *n* at which interior structures begin to appear, even if they are not global minima. The structures involving small numbers of water molecules provide insight into the microsolvation of the anions, while the fully solvated structures provide increasingly useful information about the bulk solution. Details of the computational approach are provided in Section II.

An additional motivation is to test the EFP method against the corresponding predictions of Hartree−Fock (HF) and Møller−Plesset second order perturbation theory (MP2).[51−54] The EFP method was developed for the water molecule and was designed to reproduce HF results for aqueous solvation while requiring considerably less computational cost.[1,2]

The EFP approach has been successfully applied to a variety of problems, including the solvation of small cations,[55] the solvation of the Menshutkin reaction,[56] the solvation of an S_N2 reaction,[57] and the energetics and structures of small water clusters.[58] Recently, Webb and Merrill studied the solvation of small anions ($X^-(H_2O)_n$) using the EFP method.[43] In their study, F^- and Cl^- anions were solvated by $n = 1-6$ effective fragment potentials. The EFP predictions were compared with results obtained with HF optimizations and MP2 single-point calculations. Their results suggest that interior anions do not exist for $X^-(H_2O)_n$, for $n = 1-6$. The energy differences between structures within a given cluster of size n were observed to be small. Comparisons between the present work and the results of Webb and Merrill will be given in Section III.

II. Computational Methods

Global minimum energy structure searches were performed using the HF level of theory and the 6-31++G(d,p)[59−62] basis set for X^- anions. All water molecules were treated as EFPs. The general atomic and molecular electronic structure system (GAMESS) was used for all calculations.[63]

Searches for the minimum energy structures, including the global minimum, on the $X^-(H_2O)_n$ potential energy surfaces used a Monte Carlo[64]/simulated annealing code.[65] Simulated annealing was used to initiate structure searches at 600 K and slowly cool the system to 300 K. Geometry optimizations (at 0 K) were performed after every 10 steps in the simulation. The number of EFP water molecules (*n*) was systematically increased from 1 to 15 (20) for F^- (Cl^-), to determine the smallest water cluster that fully solvates the anion as the lowest-energy species.

To characterize each stationary point that was found by the Monte Carlo searches, the Hessian (matrix of energy second derivatives) was calculated and diagonalized at each stationary point. Local minima are characterized by a positive definite Hessian. Double differencing was used to calculate the Hessians.

Single-point fully ab initio energy calculations were performed on at least the five lowest-energy structures for each value of *n*, to compare relative EFP/HF, HF, and MP2 energies for surface and interior structures. The same 6-31++G(d,p) basis set was used for the fully HF and MP2 calculations. Reported energies at all levels of theory include zero point energy (ZPE) corrections that were obtained from the Hessians

* Author to whom correspondence should be addressed. Telephone: 515-294-0452, 6342. Fax: 515-294-0105, 5204. E-mail: gordon@ameslab.gov.

10.1021/jp058086b CCC: $30.25
Published on Web 08/05/2005

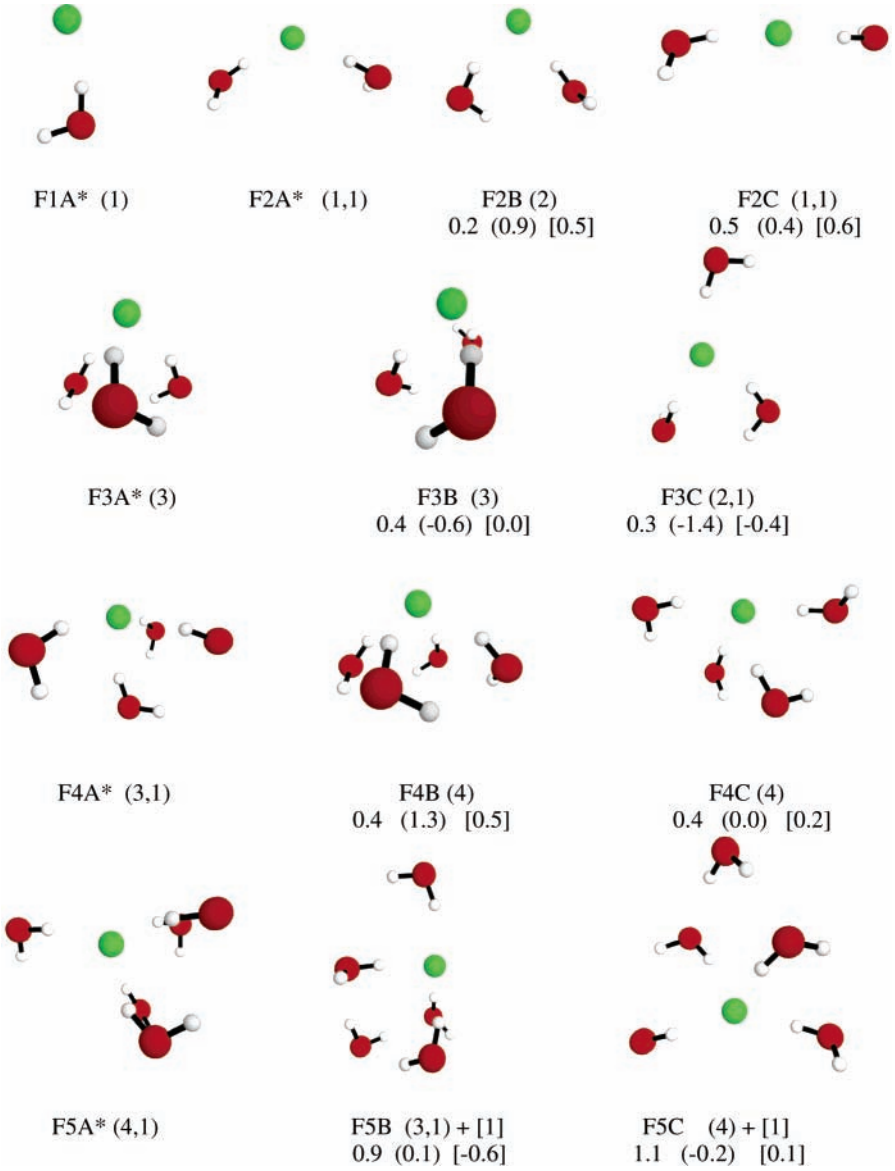

Figure 1. Local minimum structures for $F^-(H_2O)_n$ ($n = 1-5$). An asterisk (*) denotes the global minimum structure for each value of *n*. Each structure is given a unique name, X*n*I, where X is the anion present, *n* is based on the number of water molecules, and I is a unique alphabetic character. The number of hydrogen bonds present in different solvation shells is given. Relative energy differences between the higher-energy local minimum structures and the EFP global minimum are given at the EFP (HF) [MP2] level of theory. All relative energies are given in units of kcal/mol.

in which the anion was treated with HF and the EFP model described the water molecules.

In addition, MP2/6-311++(2df,p)[66,67] geometry optimizations were initiated at the equilibrium geometries found from the Monte Carlo calculations for $F^-(H_2O)_n$ (for $n = 1-4$). The criterion for convergence was 10^{-5} hartree/bohr. Hessians were calculated at these equilibrium geometries, using double differencing. Single point CCSD(T)[68,69] calculations were then performed on these optimized structures, using the same basis set.

Although a few $F^-(H_2O)_n$ and $Cl^-(H_2O)_n$ structures were found that have one imaginary frequency, the magnitude of these frequencies is small (usually <50 cm^{-1}) and they are floppy modes involving the solvent molecules. Because the Hessians are calculated using finite differences of analytic gradients, these small imaginary frequencies may be numerical noise. In any case, none of the structures with an imaginary frequency were predicted to be the lowest-energy structure by any level of theory. Therefore, the structures that have imaginary frequencies have no effect on the trend of moving from a surface anion to a completely solvated anion for either fluoride or chloride.

III. Results and Discussion

A. $F^-(H_2O)_n$, for $n = 1-15$. Global minimum structures with <11 water molecules are always surface anions. The first interior anion is observed when $n = 6$, but interior anions exist as high-energy species until $n = 12$. The Monte Carlo simulations predict that 15 water molecules are required to fully solvate the F^- anion. Calculations were also performed on the F^- anion with 17 water molecules to ensure that the solvation trend observed for groupings of 12−15 waters continues as *n* increases further. If so, the surrounded anions should also exist with larger water clusters. This is found to be the case.

Starting with the first structure in Figure 1, all structures in this paper are labeled with a unique name underneath the structure. The names for each structure follow the format X*n*I, where X represents the anion in the structure, *n* denotes the

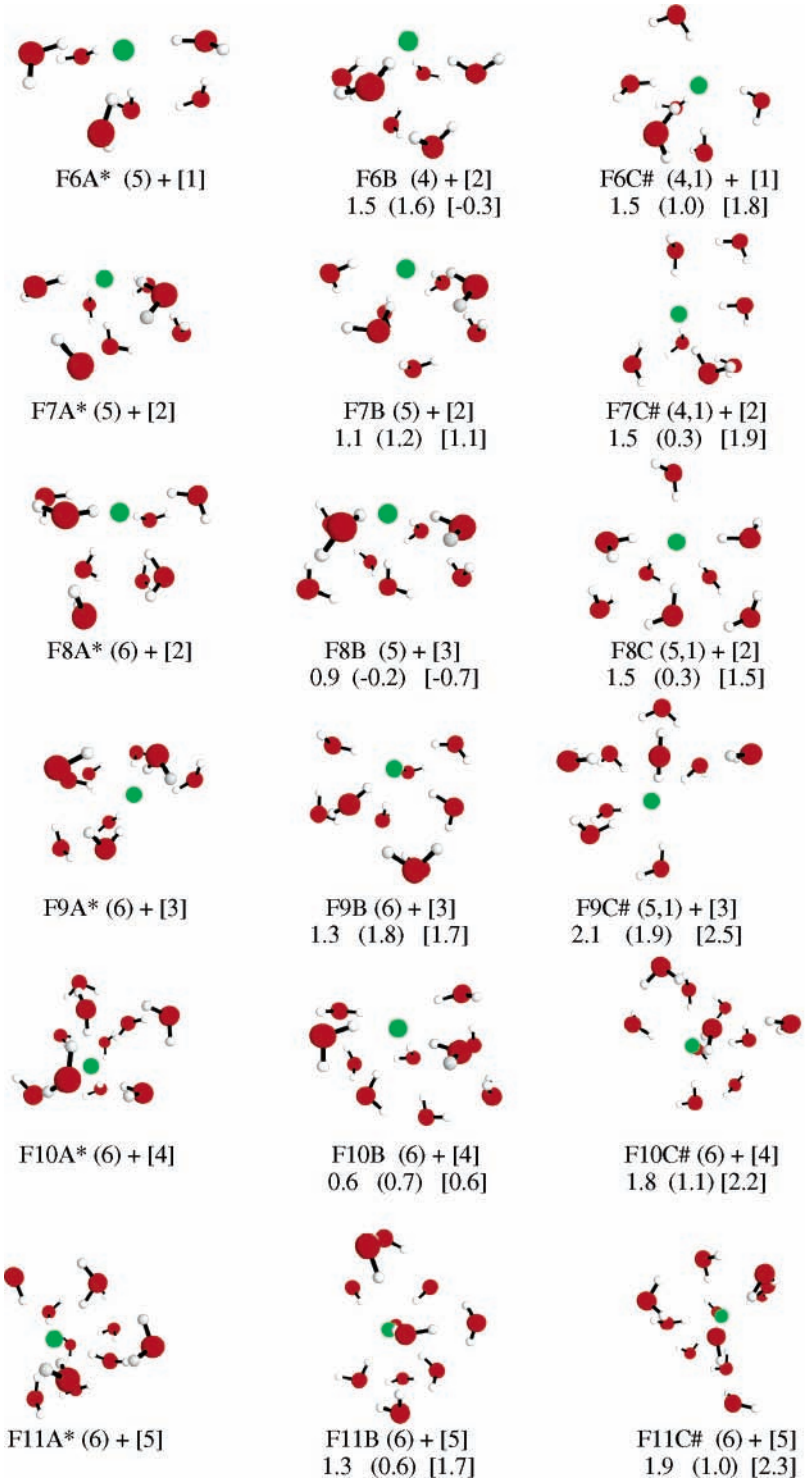

Figure 2. Local minimum structures are given for $F^-(H_2O)_n$ ($n = 6-11$). The structures in the first column are marked by an asterisk (*) and are the global minima, whereas the pound symbol (#) denotes the lowest-energy interior anion for each value of *n*.

number of water molecules present, and I is an alphabetical letter. The structures marked by a pound symbol (#) are interior anions. The structures marked with an asterisk (*) are the EFP global minimum structures. When the global minimum structure for a given value of *n* is an interior anion, the lowest-energy surface anion is marked by an ampersand (&).

Following each X*n*I designation is a nomenclature used to describe the solvation shells of the solvent environment. First solvation shell solvent molecules participate in hydrogen bonding with the solute anion, while second solvation shell molecules form hydrogen bonds with the first solvation shell molecules. Similarly, third shell molecules hydrogen bond with second-shell molecules. A number in parentheses (*x*) denotes the number of water molecules in the first shell. If separate groups of first solvation shell molecules are present, they are distinguished as (*x*,*y*), where *x* and *y* are the number of first solvation shell water molecules in the two distinct groups. Groups are considered separate if they are not within hydrogen bonding distance (2.5 Å) of each other. Similarly, the second [*x*,*y*] and third {*x*,*y*} solvation shell water molecules are indicated, if present. The total number of water molecules can be obtained by adding the number of first, second, and third shell

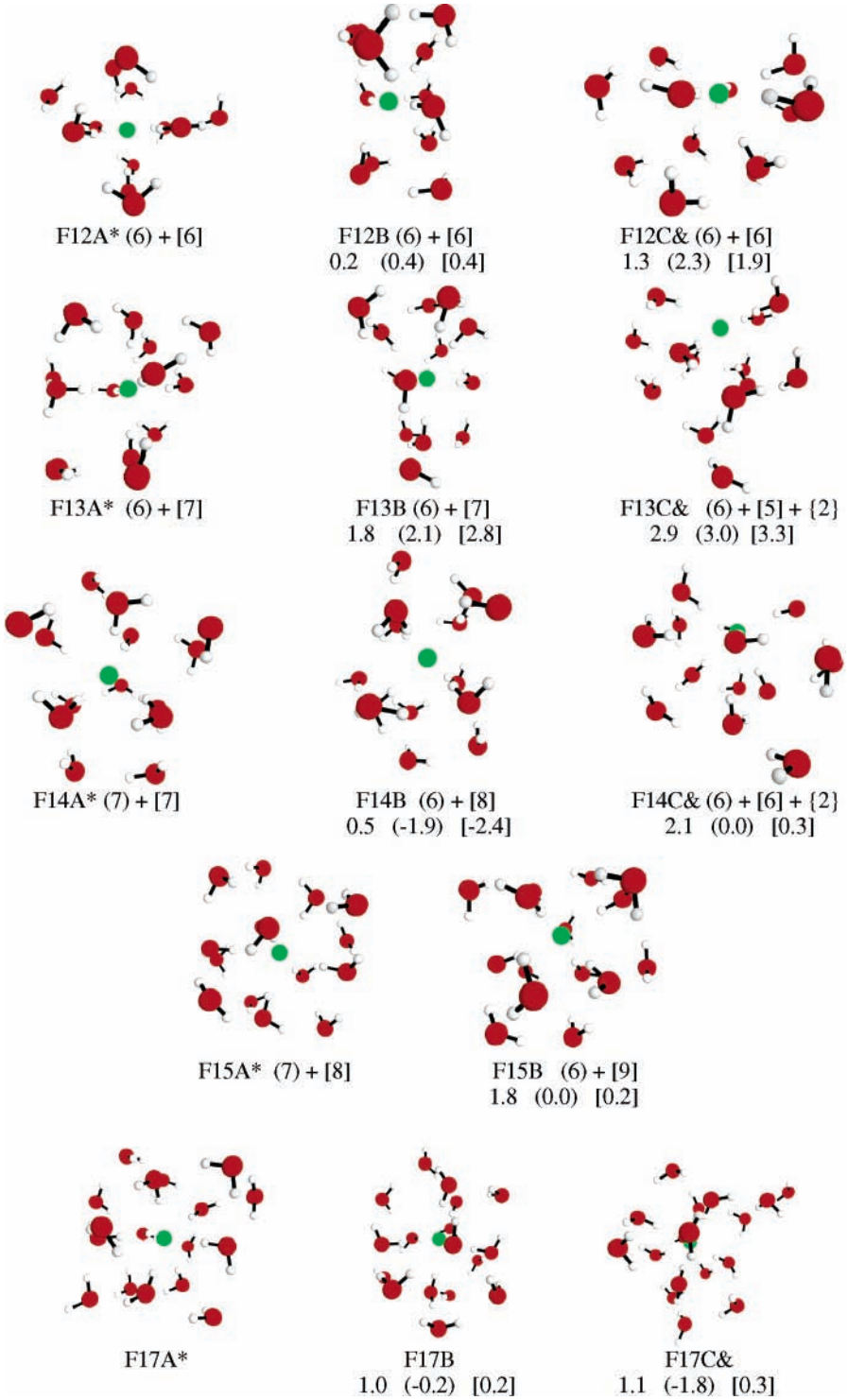

Figure 3. The structures in the first column are global minima for $F^-(H_2O)_n$ ($n = 12-15, 17$). The second column shows structures that are local minima but are higher in energy. The structures in the third column are marked by an ampersand (&) and are the lowest-energy structure that most closely resemble a surface anion. Both structures F15A* and F17A* are completely solvated.

molecules. Except for the first row in Figures 1 and 4, the structures in each row of Figures 1−8 contain the same number of water molecules (n). Each consecutive row adds one water molecule.

Below this nomenclature, the EFP (HF) and [MP2] relative energies (kcal/mol) are given in Figures 1−9. The energy difference (ΔE) between the energy E^* of the EFP global minimum structure and that of another structure (E) is obtained by subtracting E^* from E:

$$E - E^* = \Delta E \qquad (1)$$

Therefore, a positive ΔE indicates that the global minimum structure, determined using EFP waters, is more stable than the structure with energy E. A negative ΔE value indicates that the structure with energy E is more stable at the corresponding level of theory.

Local minima for $F^-(H_2O)_n$, for $n = 1-5$, are illustrated in Figure 1. Global minimum structures are given in the first column of the figure. Structures F2C, F3C, and F5C are either planar or almost planar and, therefore, cannot exist as interior anions. Therefore, interior anions do not exist for $n = 1-5$.

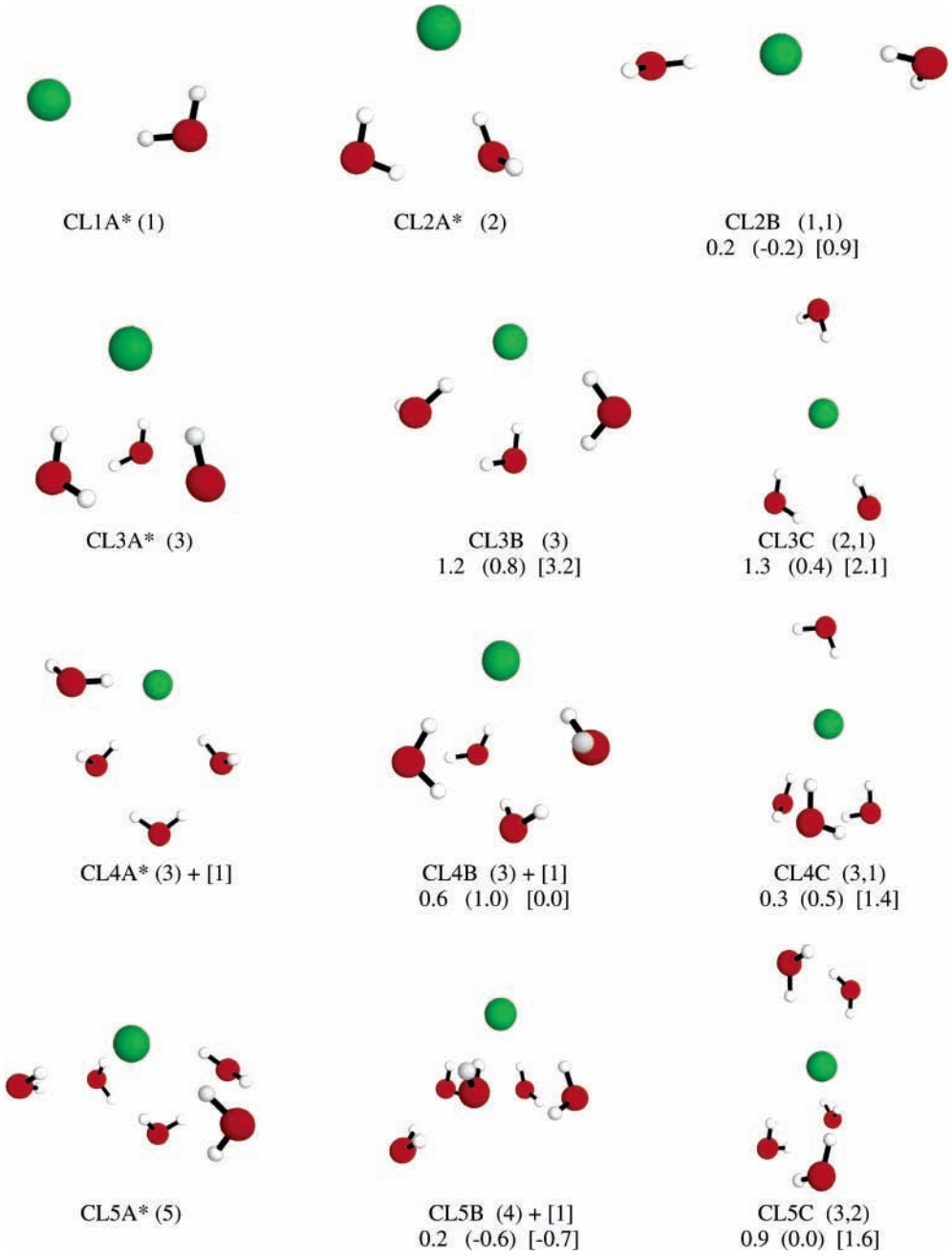

Figure 4. Local minimum structures for $Cl^-(H_2O)_n$ ($n = 1-5$). The first column represents the global minimum structure for a given value of n. The second column is a local minimum structure but is a higher-energy species than the global minimum. The structure in the third column is the lowest-energy species that most resembles an interior anion. The nomenclature used for Figures 1−3 is also used here.

Note that, for $n = 1-4$, all water molecules reside in a given hemisphere. The second column of Figure 1 presents local minima that are neither global minima nor interior structures. Generally, the relative energies predicted by EFP are in good agreement with those determined using HF or MP2 at the EFP geometries, with deviations on the order of 1 kcal/mol or less.

Figure 2 is organized similarly to Figure 1; only three structures are shown for each value of n, $n = 6-11$. Structure F6C# is the first interior structure observed; however, it is not the global minimum structure for $n = 6$. Although, in a few cases, the relative energies of the structures changes as the level of theory changes, HF and MP2 agree that the EFP global minimum is lower in energy than the lowest energy interior anion for $n = 6-11$, and the quantitative agreement among the three levels of theory is again very good, typically within 1 kcal/mol.

The EFP method suggests that the first global minimum structure that exists as an interior anion occurs for $n = 12$, F12A* in Figure 3. Figure 3 also presents the lowest energy surface anion structure in the third column. All structures are local minima, including those in the second column, which represents a higher-energy species than the global minimum. The lack of water molecules in the lower right quadrant (F12A*, F13A*, and F14A*) and the lower left quadrant (F12A* and F14A*) illustrates incomplete solvation. As for the smaller clusters, there is generally good agreement among the three levels of theory. An exception occurs for $n = 14$. Here, the EFP method predicts structure F14A* to be the global minimum, whereas HF and MP2 predict the F14B structure to be lower in energy. Both are interior structures, so the methods are in qualitative agreement.

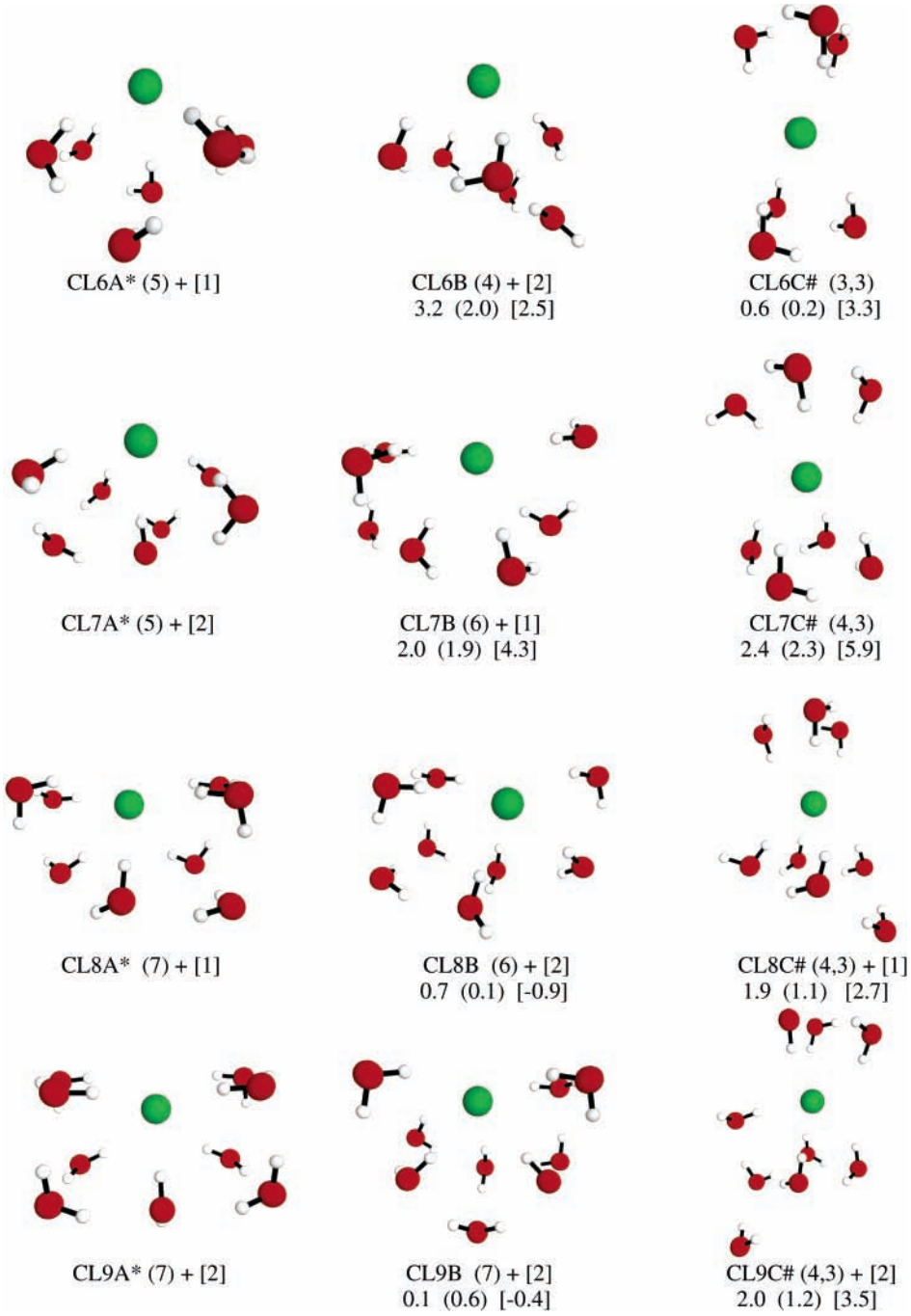

Figure 5. Local minimum structures for $Cl^-(H_2O)_n$ ($n = 6-9$). The first column shows the global minimum structure for a given value of n. The second column is a local minimum structure but is a higher-energy species than the structure in the first column. The third column represents the lowest-energy interior anion structures.

The global minimum structure for $n = 15$ (F15A* in Figure 3) is completely solvated. Unlike $n = 12-14$, every quadrant in structure 15A* has approximately the same concentration of water molecules. The other structure for $n = 15$ (F15B) is the lowest-energy structure for $n = 15$ that is not completely solvated. This solvation trend continues for $n = 17$, for which the global minimum structure is F17A*.

The structures presented here generally agree with those of Webb and Merrill.[43] However, their study did not explicitly seek the global minimum structure. Instead, they optimized structures that were previously presented in the literature. These authors predict EFP, HF, and MP2 structures with two distinct groups of waters in the first solvation shell to be the lowest-energy species for $n = 2$, 4, and 5 (EFP, HF, and MP2). The global minimum structure found by the Monte Carlo calculations reported here for $n = 5$ is composed of two groups of water molecules, one of which appears to reside in a second solvation shell. For $n = 6$ (EFP, HF, and MP2), both the results of the Monte Carlo calculations and those of Webb and Merrill predict a single group of first solvation shell molecules in the global minimum structure. The small energy differences between the structures given in Figures 1−3 are in good agreement with the results of Webb and Merrill.

B. $Cl^-(H_2O)_n$, for $n = 1-18$. Monte Carlo calculations predict that no fewer than 18 water molecules are required to completely solvate the Cl^- anion. Monte Carlo calculations were also performed with the Cl^- anion and a water cluster with 20 water molecules to confirm the findings for $n = 18$. Global

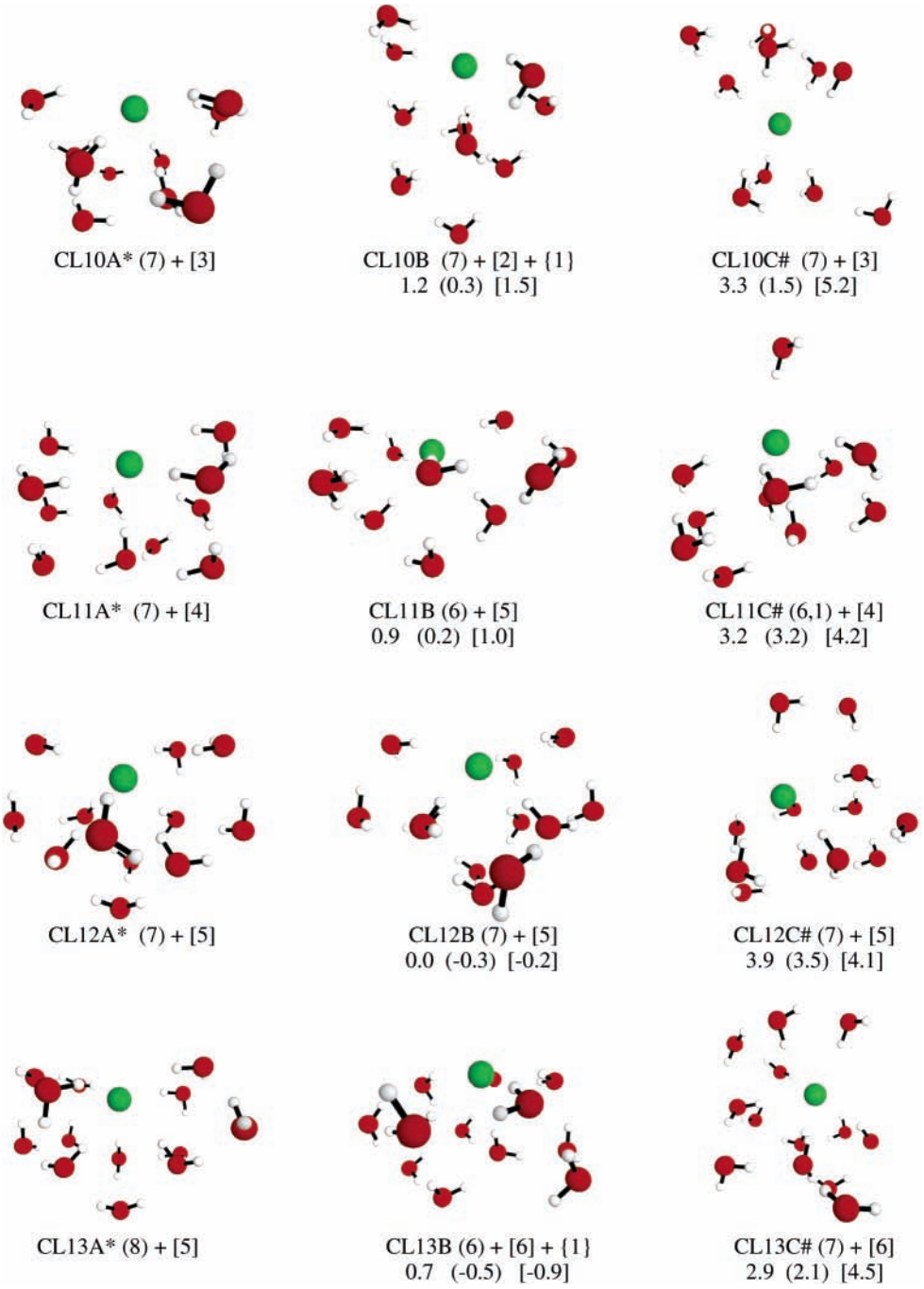

Figure 6. Local minimum structures for $Cl^-(H_2O)_n$ ($n = 10-13$). The same nomenclature and format of Figure 5 is used here. Although interior anions exist for each value of n, none of these are the global minimum structure.

minima for $Cl^-(H_2O)_n$ are given in Figures 4−8 in the left-hand column. The same nomenclature as that for the F^- anion is used.

The second column in Figures 4−8 presents a higher-energy local minimum. The structures that most resemble an interior anion structure for $n = 1-5$ are given in the third column of Figure 4. Structures CL2B and CL3C are planar, while structures CL4C and CL5C have a large space without water molecules located toward the right-hand side of each structure. While these structures are closest to being an interior anion for $n = 2-5$, they are actually surface anions. This is similar to the results found for F^-. The global minima obtained for $Cl^-(H_2O)_n$ (for $n = 1-6$) are in good agreement with the results of Webb and Merrill at all levels of theory.[43] No interior anions were observed for $n = 1-5$ by either the Monte Carlo calculations or Webb and Merrill. The relative energies predicted by the three levels of theory are in good agreement with each other.

Figures 5−7 give local minima for $Cl^-(H_2O)_n$ (for $n = 6-17$). As for F^-, the first interior anions are observed for $Cl^-(H_2O)_n$ when $n = 6$; the lowest-energy example is given in the third column of Figure 5. As the water cluster size grows, the anion approaches complete solvation. The interior anions do not exist as global minima until the completely solvated structure is found ($n = 18$). Recall the global minima in Figure 3 for examples of interior anions. Somewhat greater disagreement among the three levels of theory is observed for Cl^- than for F^-. Disparities as large as 2−3 kcal/mol are found for CL7B and CL7C#, for example. In nearly all cases, EFP and HF are in good agreement, whereas these two methods deviate somewhat from the MP2 relative energies. Therefore, these errors

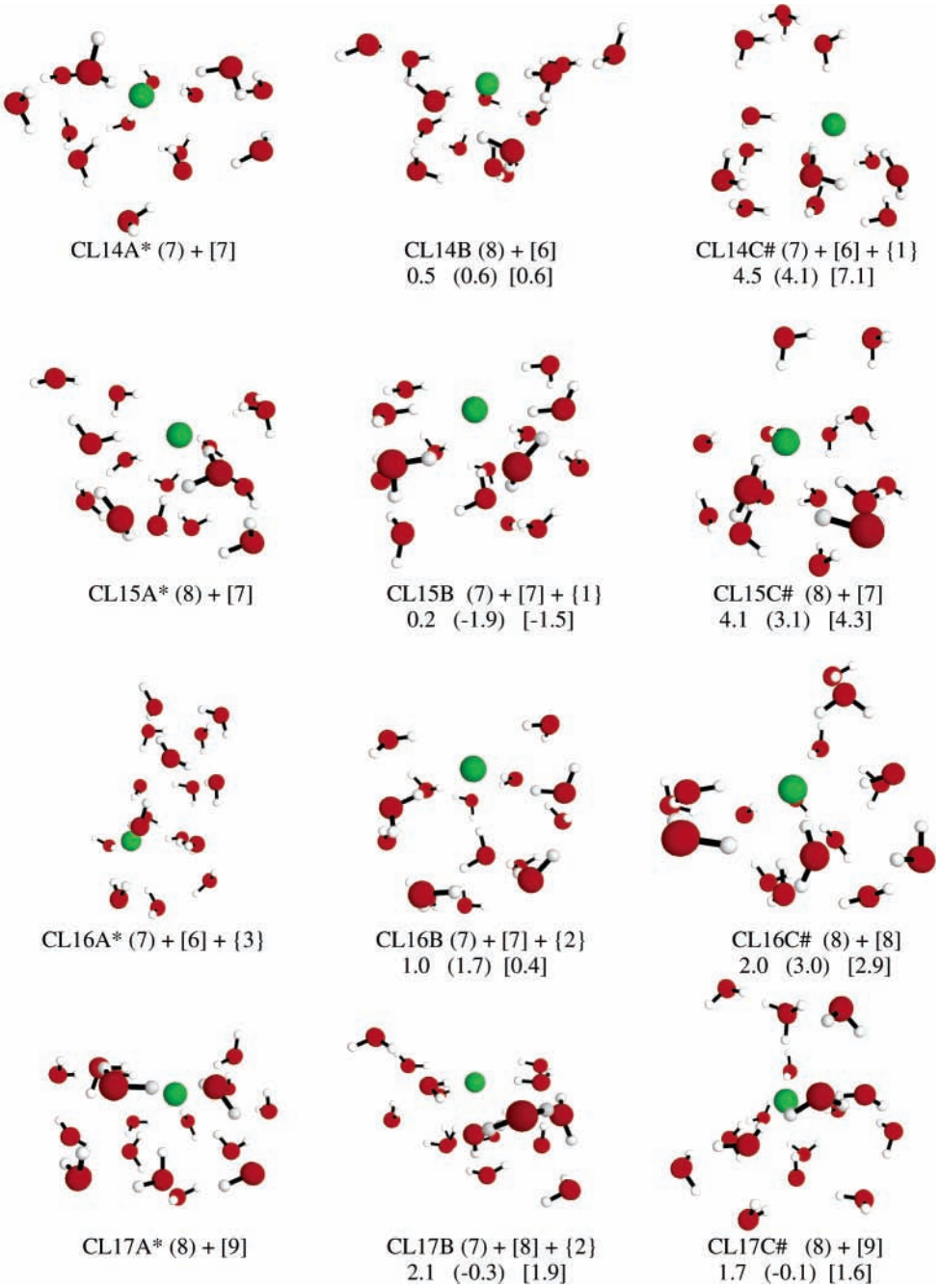

Figure 7. Three structures for $Cl^-(H_2O)_n$ ($n = 14-17$). The same nomenclature and format of Figures 5 and 6 are used here again. As with the smaller clusters, none of the interior anions are global minimum structures.

result from deficiencies in the HF method, from which this EFP method is derived, and are not inherent in the EFP approach itself. Nonetheless, the three methods do consistently predict similar trends with regard to the relative stabilities of interior versus exterior structures.

Positive relative energies for $n = 18$ illustrate the stability of the fully solvated anion, relative to the partially solvated anion. HF and MP2 single-point energies at the five lowest EFP structures for $Cl^-(H_2O)_{18}$ predict that the global minimum is the completely solvated CL18A* structure (see Figure 8). The EFP, HF, and MP2 relative energies predict a fully solvated anion to be lower in energy by 4.3, 1.8, and 4.2 kcal/mol, respectively. The HF and MP2 single points at the five lowest EFP structures for $n = 20$ suggest a completely solvated anion to be more stable than a partially solvated anion by 1.3 (EFP), 2.1 (HF), and 4.2 (MP2) kcal/mol.

Larger energy differences between interior and surface anions are observed for $Cl^-(H_2O)_n$ than for $F^-(H_2O)_n$. The source of these higher-energy differences may be the fact that Cl^- resists becoming an interior anion until complete solvation is obtained at $n = 18$. Comparing the experimental differential binding energies for each anion in Tables 1 and 2 shows that small water clusters are more tightly bound to F^- than to Cl^-. The strong interaction between F^- and water molecules is likely to encourage interactions between the water cluster and the anion, resulting in interior anions that are relatively lower in energy than the analogous chloride structures.

C. Binding Energies. Binding energies and differential binding energies were calculated for $F^-(H_2O)_n$ (for $n = 1-15$) and $Cl^-(H_2O)_n$ (for $n = 1-18$) at the EFP/HF, HF, and MP2 levels of theory. Boltzmann-averaged energies were calculated

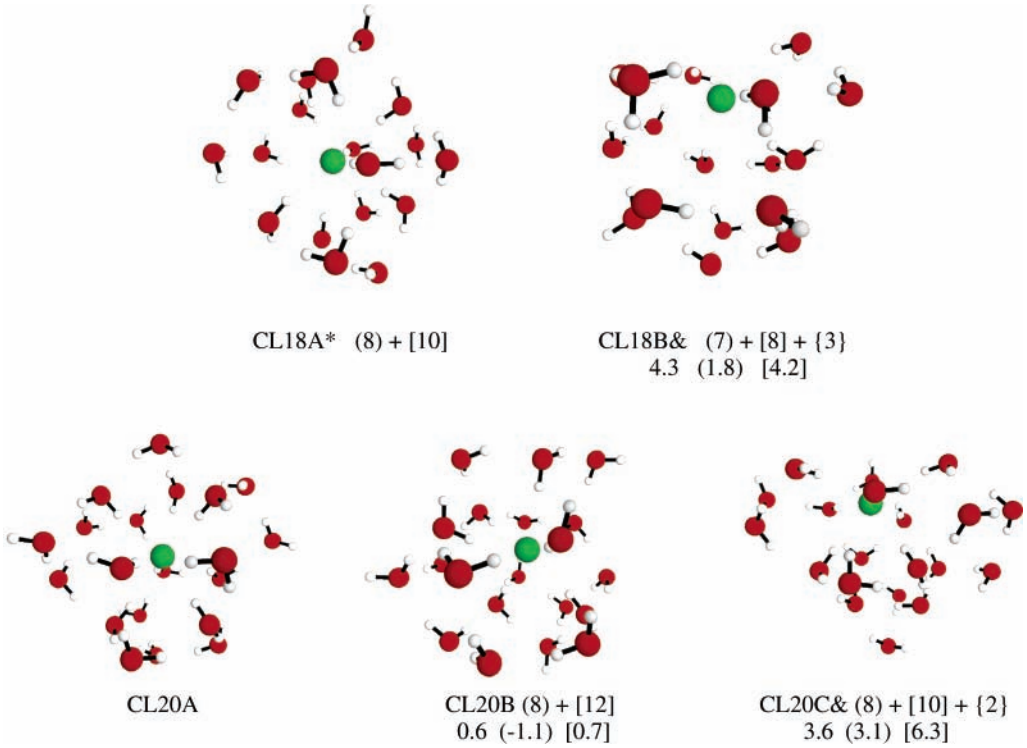

Figure 8. Local minima for $Cl^-(H_2O)_n$ ($n = 18$, 20). The global minima for $n = 18$ and $n = 20$ are interior anions and are completely solvated. The relative energies between the global minimum and the lowest-energy surface anion is larger for $n = 20$. The structures in the last column are marked by an ampersand (&) and are the lowest-energy structures that are not completely solvated.

TABLE 1: Differential Binding Energies for $F^-(H_2O)_n$, Given at the EFP, HF, and MP2 Levels of Theory

	Experiment[a]	EFP/HF			HF			MP2		
number of water molecules	binding energy (kcal/mol)	binding energy (kcal/mol)	error[b] (kcal/mol)	% error[c]	binding energy (kcal/mol)	error[b] (kcal/mol)	% error[c]	binding energy (kcal/mol)	error[b] (kcal/mol)	% error[c]
1	−23.3	−17.3	6.0	25.7	−20.2	3.1	13.5	−20.8	2.5	10.7
2	−19.2	−15.3	3.9	20.1	−17.2	2.0	10.3	−17.9	1.3	6.6
3	−15.3	−14.0	1.3	8.8	−14.1	1.2	7.6	−15.3	0.0	0.2
4	−13.9	−12.4	1.5	11.0	−11.4	2.5	18.0	−13.2	0.7	4.8
5	−12.3	−10.1	2.2	18.2	−10.1	2.2	17.8	−12.6	−0.3	−2.3
6	−10.9	−10.0	0.9	8.3	−8.5	2.4	21.7	−11.6	−0.7	−6.8
7	−10.4	−10.7	−0.3	−2.8	−9.2	1.2	11.9	−12.0	−1.6	−15.8
8	−11.2	−9.6	1.6	14.6	−8.5	2.7	24.1	−10.9	0.3	2.4
9	−11.1	−7.9	3.2	28.5	−7.4	3.7	33.5	−9.3	1.8	16.5
10		−9.7			−8.4			−11.7		
11		−7.3			−7.1			−9.9		
12		−8.7			−8.6			−11.0		
13		−9.1			−7.8			−11.5		
14		−8.3			−6.6			−11.0		
15		−8.6			−5.7			−8.5		

[a] Data taken from refs 70 and 71. [b] The error columns were obtained by taking the difference between the predicted value for a given value of n and the experimental value. [c] Percent errors were calculated by dividing the error column by the experimental column and multiplying by 100.

for each water cluster, using the Boltzmann equation:

$$\frac{\sum_i X_i \, e^{-\Delta E_i/(RT)}}{\sum_i e^{-\Delta E_i/(RT)}} = E_n \qquad (2)$$

where X_i is the calculated energy of the ith structure, including a zero point vibrational energy correction (obtained from the EFP/HF Hessians). ΔE_i is calculated by taking the difference between the energy of the ith structure and the lowest-energy structure of a given cluster of n water molecules ($T = 298$ K). The result (E_n) is the Boltzmann-averaged energy for all structures composed of n water molecules.

The differential binding energy is defined as the energy difference for the following process:

$$\Delta D_e = X^-(H_2O)_n + H_2O \rightarrow X^-(H_2O)_{n+1} \qquad (3)$$

where $X = F^-$ (Cl^-) and $n = 0-14$ (0−17). The differential binding energies were calculated by taking the Boltzmann-averaged energy for $X^-(H_2O)_{n+1}$ and subtracting it from the sum of the Boltzmann-averaged energy for $X^-(H_2O)_n$ and the energy of one water molecule. The calculated differential binding energies are compared with available experimental values in Tables 1 and 2.

The total binding energy is

$$D_e = X^- + nH_2O \rightarrow X^-(H_2O)_n \qquad (4)$$

The binding energies were calculated by taking the sum of the

TABLE 2: Differential Binding Energies for $Cl^-(H_2O)_n$, Given at the EFP, HF, and MP2 Levels of Theory[a]

	Experiment	EFP/HF			HF			MP2		
number of water molecules	binding energy (kcal/mol)	binding energy (kcal/mol)	error[b] (kcal/mol)	% error	binding energy (kcal/mol)	error[b] (kcal/mol)	% error	binding energy (kcal/mol)	error[b] (kcal/mol)	% error
1	−14.7	−10.8	3.9	26.2	−10.4	4.3	29.0	−12.4	2.3	15.8
2	−13.0	−10.3	2.7	20.5	−9.5	3.5	27.2	−11.7	1.3	9.7
3	−11.8	−10.6	1.2	10.2	−9.0	2.8	24.1	−12.3	−0.5	−4.4
4	−10.6	−9.1	1.5	14.2	−8.8	1.8	17.1	−10.7	−0.1	−1.3
5	−9.5	−8.3	1.2	12.2	−6.6	2.9	30.7	−9.5	0.0	0.3
6	−8.8	−10.1	−1.3	−14.3	−8.2	0.6	7.3	−12.2	−3.4	−38.9
7		−8.7			−7.9			−10.6		
8		−6.5			−5.3			−7.6		
9		−8.6			−7.1			−10.0		
10		−7.4			−5.7			−8.1		
11		−9.7			−9.1			−12.3		
12		−7.8			−6.2			−9.1		
13		−6.6			−6.1			−9.6		
14		−7.3			−6.7			−9.0		
15		−6.5			−5.6			−8.5		
16		−8.0			−7.0			−9.7		
17		−8.7			−5.4			−9.9		
18		−8.6			−7.3			−12.8		

[a] Experimental data taken from ref 70. [b] The error columns were obtained by taking the difference between the predicted value for a given value of *n* and the experimental values.

TABLE 3: Total Binding Energies for $F^-(H_2O)_n$, Given at the EFP, HF, and MP2 Levels of Theory

	Experiment[a]	EFP/HF			HF			MP2		
number of water molecules	binding energy (kcal/mol)	binding energy (kcal/mol)	error[b] (kcal/mol)	% error[c]	binding energy (kcal/mol)	error[b] (kcal/mol)	% error[c]	binding energy (kcal/mol)	error[b] (kcal/mol)	% error[c]
1	−23.3	−17.3	6.0	25.7	−20.2	3.1	13.5	−20.8	2.5	10.7
2	−42.5	−32.7	9.8	23.2	−37.4	5.1	12.0	−38.7	3.8	8.9
3	−57.8	−46.6	11.2	19.4	−51.5	6.3	10.9	−54.0	3.8	6.6
4	−71.7	−59.0	12.7	17.7	−62.9	8.8	12.3	−67.2	4.5	6.2
5	−84.0	−69.0	15.0	17.8	−73.0	11.0	13.1	−79.8	4.2	5.0
6	−94.9	−79.0	15.9	16.7	−81.6	13.3	14.1	−91.5	3.4	3.6
7	−105.3	−89.7	15.6	14.8	−90.7	14.6	13.8	−103.5	1.8	1.7
8	−116.5	−99.3	17.2	14.8	−99.2	17.3	14.8	−114.4	2.1	1.8
9	−127.6	−107.2	20.4	16.0	−106.6	21.0	16.5	−123.7	3.9	3.0
10		−116.9			−115.0			−135.4		
11		−124.2			−122.1			−145.3		
12		−132.9			−130.7			−156.3		
13		−142.1			−138.5			−167.7		
14		−150.3			−145.1			−178.7		
15		−159.0			−150.8			−187.2		
17		−171.4			−162.1			−203.8		

[a] Data taken from refs 70 and 71. [b] The error columns were obtained by taking the difference between the predicted value for a given value of *n* and the experimental value. [c] Percent errors were calculated by dividing the error column by the experimental column and multiplying by 100.

TABLE 4: Total Binding Energies for $Cl^-(H_2O)_n$ at the EFP, HF, and MP2 Levels of Theory

	Experiment	EFP/HF			HF			MP2		
number of water molecules	binding energy (kcal/mol)	binding energy (kcal/mol)	error[b] (kcal/mol)	% error	binding energy (kcal/mol)	error[b] (kcal/mol)	% error	binding energy (kcal/mol)	error[b] (kcal/mol)	% error
1	−14.7	−10.8	3.9	−26.2	−10.4	4.3	−29.0	−12.4	2.3	−15.8
2	−27.7	−21.2	6.5	−23.5	−19.9	7.8	−28.2	−24.1	3.6	−12.9
3	−39.5	−31.8	7.7	−19.6	−28.9	10.6	−26.9	−36.4	3.1	−7.8
4	−50.1	−40.9	9.2	−18.4	−37.6	12.5	−24.9	−47.2	2.9	−5.8
5	−59.6	−49.2	10.4	−17.4	−44.2	15.4	−25.8	−56.7	2.9	−4.9
6	−68.4	−59.3	9.1	−13.3	−52.4	16.0	−23.4	−68.9	−0.5	0.7
7		−68.0			−60.2			−79.5		
8		−74.4			−65.5			−87.1		
9		−83.0			−72.6			−97.1		
10		−90.5			−78.3			−105.2		
11		−100.1			−87.3			−117.5		
12		−107.9			−93.6			−126.6		
13		−114.5			−99.6			−136.2		
14		−121.8			−106.3			−145.2		
15		−128.3			−111.9			−153.7		
16		−136.3			−118.9			−163.4		
17		−145.0			−124.4			−173.3		
18		−153.6			−131.7			−186.0		
20		−169.2			−146.2			−206.7		

[a] Experimental data taken from ref 70. [b] The error columns were obtained by taking the difference between the predicted value for a given value of *n* and the experimental value.

energy of the anion and *n* water molecules and subtracting it from the Boltzmann-averaged energy for the $X^-(H_2O)_n$ system. The results of these calculations are given in Tables 3 and 4.

Both the experimental and calculated differential binding energies generally decrease with increasing *n*. For the Cl^- anion, the experimental values decrease monotonically, through $n = 6$, while some fluctuations are observed for all of the computed ΔD_e values. For F^-, some fluctuations are observed for both

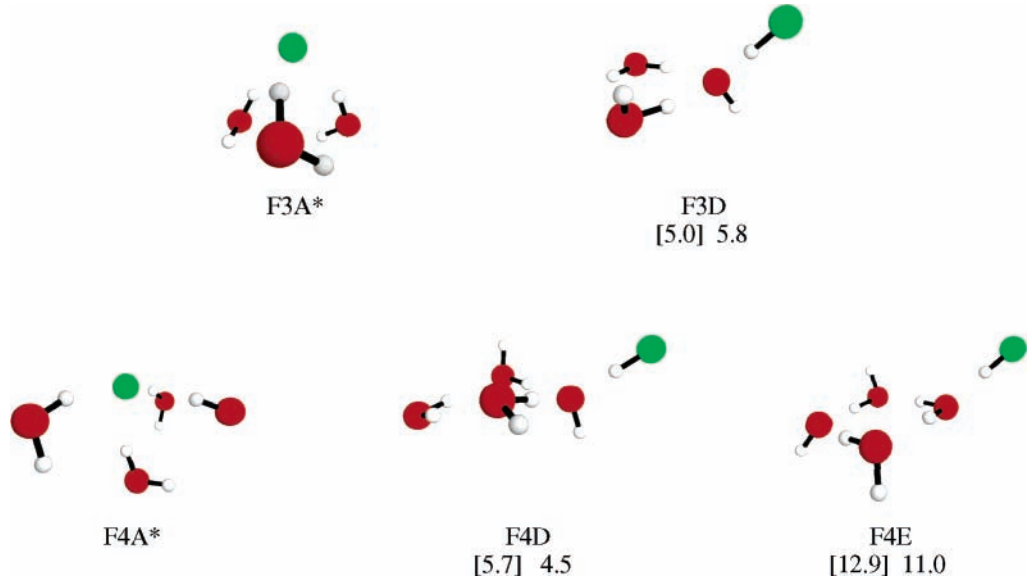

Figure 9. $F^-(H_2O)_n$ ($n = 3, 4$) structures (left) are compared with the $HF + OH^- + nH_2O$ ($n = 2, 3$) structures. The solvated fluoride structure is the global minimum in both cases and is marked by an asterisk (*). Relative energy differences, in units of kcal/mol, are given at the [MP2] and CCSD(T) levels of theory.

experiment and theory. The fluctuations are not consistent enough to be explained by obvious structural differences for the smaller clusters.

The most surprising fluctuation occurs for $Cl^-(H_2O)_{18}$, for which MP2 predicts that the 18th water molecule is more tightly bound than the first! It may be that the unexpectedly high differential binding energy for $n = 18$ is due to the fact that the 18th water molecule enables the water cluster to form an interior anion and completely solvate the Cl^- anion. Although there is a smaller fluctuation at the HF level from $n = 17$ to $n = 18$, no significant fluctuation exists for EFP. Similar fluctuations were found by Webb and Merrill, for small values of n.

With some exceptions, the error in differential binding energies decreases as n increases; therefore, the percent error is approximately constant. The HF errors are somewhat larger than those found for the EFP method while, not surprisingly, MP2 is in the best agreement with experiment.

In general, the HF and EFP total binding energies are in good agreement with each other, with errors of ~15%−25%, relative to the experimental values. Thus, once again, errors in the EFP predictions most likely reflect inadequacies in the underlying HF method upon which the EFP parametrization is based,[1,2] rather than on any inherent failing of the EFP method itself. Both methods exhibit the correct qualitative trends, when compared with the experiment, but have significant quantitative errors. However, the MP2 total binding energies agree both quantitatively and qualitatively with experiment, suggesting the importance of dynamic correlation.

D. Comparison between $F^-(H_2O)_n$ and $HF(OH^-)(H_2O)_{n-1}$. In order to further assess the reliability of the EFP method, MP2 geometry optimizations were performed on the lowest-energy structures for $F^-(H_2O)_n$ ($n = 1-4$). Since the EFP method[1,2] freezes the internal coordinates of the water molecule, it is important to determine the impact of this approximation. In the fully MP2 optimizations, the internal coordinates of the water molecules were not constrained.

The MP2 optimizations explored both $F^-(H_2O)_n$ (for $n = 1-4$) and $HF + OH^- + (n-1)H_2O$. The latter system could be formed from the former if the F^- anion extracts a proton from one of the water molecules. If $HF + OH^- + (n-1)H_2O$ is the global minimum, especially if $F^-(H_2O)_n$ is not even a local minimum, the EFP method would be less meaningful for those values of n.

The MP2 potential energy surface of $F^-(H_2O)$ was calculated previously by Janoschek,[37] who chose a 6-311+G(2df,p)[66,67] basis set. For consistency, the 6-311++G(2df,p) basis set was used. The optimized MP2 structure for $F^-(H_2O)$ agrees well with the global minimum found by Janoschek. $HF(OH^-)$ is not a minimum on the potential energy surface. The formation of HF is first observed when two water molecules are present to stabilize its coexistence with OH^-. The resulting equilibrium geometry, F3D in Figure 9, is a local minimum. At the CCSD(T)//MP2 level of theory, this local minimum is 5.8 kcal/mol above the $F^-(H_2O)_3$ global minimum. The HF bond distance in F3D is 1.06 Å, whereas that of an unsolvated HF molecule is 0.96 Å. Thus, the HF bond is stretched because of the presence of the OH^- anion.

Two local minima for $HF + OH^- + 3H_2O$ are shown in Figure 9. One structure involves a hydrogen bond between HF and hydroxide (structure F4D), whereas the other involves a hydrogen bond between HF and a water molecule (F4E). At the CCSD(T) level of theory, structure F4D (F4E) is 4.5 (11.0) kcal/mol higher than the solvated F^- anion shown as structure F4A in Figure 9.

These results suggest that, although $HF + OH^-$ does coexist with solvated F^-, they are higher on the potential energy surface. Therefore, using frozen internal coordinates in the EFP method is reasonable for studying the solvated anions, because protons are not easily extracted from the water molecules.

IV. Conclusions

The effective fragment potential (EFP) method, coupled with Monte Carlo simulations, was applied to study the solvation of F^- and Cl^- anions. The method provides a reliable approach for analyzing anion solvation. The EFP, HF, and MP2 calculations predict that no fewer than 15 water molecules are required to fully solvate a single F^- anion. All three levels of theory predict that 18 water molecules are required for complete solvation of the Cl^- anion. The frozen internal coordinates of the EFP are appropriate for studying small water clusters in the presence of F^- anions, since proton transfer from a water

molecule to the anion is not favored thermodynamically. It is important to keep in mind, of course, that these results are based on electronic energies at 0 K. It is possible that the incorporation of temperature and entropic effects could modify the number of waters needed to make interior anions most favorable.

All three levels of theory predict the correct qualitative trends for both total and differential binding energies. MP2 binding energies are quantitatively accurate for both the F^- and Cl^- anions, when compared to experimental values. EFP and HF errors are similar, suggesting that these errors are inherent in the HF method, from which this version of the EFP method is derived. Chloride differential binding energies fluctuate as a function of *n* for all levels of theory. The largest error in almost all cases results from the binding of the first water molecule to the anion.

Acknowledgment. Funding for this study was provided by an NSF REU program, the Air Force Office of Scientific Research, and the Iowa State University Chemistry Department. Several helpful discussions with Drs. Simon Webb and Grant Merrill are gratefully acknowledged. The authors would also like to thank Professor Tony Haymet for suggesting this project and Professor Benny Gerber for helpful discussions.

References and Notes

(1) Day, P. N.; Jensen, J. H.; Gordon, M. S.; Webb, S. P.; Stevens, W. J.; Krauss, M.; Garmer, D.; Basch, H.; Cohen, D. *J. Chem. Phys.* **1996**, *105*, 1968.
(2) Gordon, M. S.; Freitag, M. A.; Bandyopadhyay, P.; Jensen, J. H.; Kairys, V.; Stevens, W. J. *J. Phys. Chem. A* **2001**, *105*, 293.
(3) Hall, R. J.; Hillier, I. H.; Vincent, M. A. *Chem. Phys. Lett*. **2000**, *320*, 139.
(4) Majumdar, D.; Kim, J.; Kim, K. S. *J. Chem. Phys*. **2000**, *112*, 101.
(5) Vaughn, S. J.; Akhmatskaya, E. V.; Vincent, M. A.; Masters, A. J.; Hillier, I. H. *J. Chem. Phys.* **1999**, *110*, 4338.
(6) Baik, J.; Kim, J.; Majumdar, D.; Kim, K. S. *J. Chem. Phys*. **1999**, *110*, 9116.
(7) Bryce, R. A.; Vincent, M. A.; Hillier, I. H. *J. Phys. Chem*. **1999**, *103*, 4094.
(8) Xantheas, S. S.; Dunning, T. H., Jr. *J. Phys. Chem.* **1994**, *98*, 13489.
(9) Hobza, P.; Sauer, J. *Theor. Chim. Acta* **1984**, *65*, 279.
(10) Kim, J.; Lee, H. M.; Suh, S. B.; Majumdar, D.; Kim, K. S. *J. Chem. Phys*. **2000**, *113*, 5259.
(11) Gamba, A.; Manunza, B.; Gatti, C.; Simonetta, M. *Theor. Chim. Acta* **1983**, *63*, 245.
(12) Probst, M. M.; Rode, B. M. *J. Mol. Struct. (THEOCHEM)* **1982**, *88*, 91.
(13) Cabarcos, O. M.; Weinheimer, C. J.; Lisy, J. M.; Xantheas, S. S. *J. Chem. Phys*. **1999**, *110*, 5.
(14) Gora, R. W.; Roszak, S.; Leszczynski, J. *Chem. Phys. Lett*. **2000**, *325*, 7.
(15) Choi, J.; Kuwata, K. T.; Cao, Y.; Okumura, M. *J. Phys. Chem. A* **1998**, *102*, 503.
(16) Truong, T. N.; Stefanovich, E. V. *Chem. Phys. Lett.* **1996**, *256*, 348.
(17) Xantheas, S. S. *J. Phys. Chem*. **1996**, *100*, 9703.
(18) Schindler, T.; Berg, C.; Niedner-Schatteburg, G.; Bondybey, V. E. *J. Phys. Chem*. **1995**, *99*, 12434.
(19) Combariza, J. E.; Kestner, N. R.; Jortner, J. *J. Chem. Phys*. **1994**, *100*, 2851.
(20) Asada, T.; Nishimoto, K.; Kitaura, K. *J. Phys. Chem.* **1993**, *97*, 7724.
(21) Foresman, J. B.; Brooks, C. L., III. *J. Chem. Phys*. **1987**, *87*, 5892.
(22) Chaban, G. M.; Jung, J. O.; Gerber, R. B. *J. Phys. Chem. A* **2000**, *104*, 2772.
(23) Morita, A.; Hynes, J. T. *Chem. Phys*. **2000**, *258*, 371.
(24) Topol, I. A.; Tawa, G. J.; Burt, S. K. *J. Chem. Phys*. **1999**, *111*, 10998.
(25) Combariza, J. E.; Kestner, N. R. *J. Phys. Chem*. **1995**, *99*, 2717.
(26) Caldwell, J. W.; Kollmar, P. A. *J. Phys. Chem*. **1992**, *96*, 8249.
(27) Kistenmacher, H.; Popkie, H.; Clementi, E. *J. Chem. Phys*. **1973**, *59*, 5842.
(28) Xantheas, S. S.; Dang, L. X. *J. Phys. Chem*. **1996**, *100*, 3989.
(29) Zhao, X. G.; Gonzalez-Lafont, A.; Truhlar, D. G.; Stecker, R. *J. Chem. Phys*. **1991**, *94*, 5544.
(30) Tobias, D. J.; Jungwirth, P.; Parrinello, M. *J. Chem. Phys*. **2001**, *114*, 7036.
(31) Lee, H. M.; Kim, D.; Kim, K. S. *J. Chem. Phys.* **2002**, *116*, 5509.
(32) Perera, L.; Berkowitz, M. L. *J. Chem. Phys*. **1994**, *100*, 3085.
(33) Dang, L. X. *J. Chem. Phys*. **1992**, *96*, 6970.
(34) Cabarcos, O. M.; Weinheimer, C. J.; Lisy, J. M.; Xantheas, S. S. *J. Chem. Phys.* **1999**, *110*, 5.
(35) Jorgensen, W. L.; Severance, D. L. *J. Chem. Phys*. **1993**, *99*, 4233.
(36) Gao, J.; Garner, D. S.; Jorgensen, W. L. *J. Am. Chem. Soc*. **1986**, *108*, 4784.
(37) Janoschek, R. *Mol. Phys*. **1996**, *89*, 1301.
(38) Perera, L.; Berkowitz, M. L. *J. Chem. Phys*. **1991**, *95*, 1954.
(39) Yoo, S.; Lei, Y. A.; Zeng, X. C. *J. Chem. Phys*. **2003**, *119*, 6083.
(40) Heuft, J. M.; Meijer, E. J. *J. Chem. Phys*. **2003**, *119*, 11788.
(41) Ayala, R.; Martinez, J. M.; Pappalardo, R. R.; Marcos, E. S. *J. Chem. Phys*. **2003**, *119*, 9538.
(42) Jungwirth, P.; Tobias, D. J. *J. Phys. Chem. A* **2002**, *106*, 379.
(43) Merrill, G. N.; Webb, S. P. *J. Phys. Chem. A* **2003**, *107*, 7852.
(44) Heuft, J. M.; Meijer, E. J. *J. Chem. Phys.* **2005**, *122*, 094501.
(45) Heuft, J. M.; Meijer, E. J. *J. Chem. Phys.* **2003**, *119*, 11788.
(46) Hagberg, D.; Brdarski, S.; Karlström, G. *J. Phys. Chem. B* **2005**, *109*, 4111.
(47) Ayala, R.; Martinez, J. M.; Pappalardo, R. R.; Marcos, E. S. *J. Chem. Phys.* **2004**, *121*, 7269.
(48) Perera, L.; Berkowitz, M. L. *J. Chem. Phys.* **1992**, *96*, 8288.
(49) Markovich, G.; Giniger, R.; Levin, M.; Cheshnovsky, O. *Z. Phys. D: At., Mol. Clusters* **1991**, *20*, 69−72.
(50) Markovich, G.; Pollack, S.; Giniger, R.; Cheshnovsky, O. *J. Chem. Phys.* **1994**, *101*, 9344.
(51) Pople, J. A.; Binkley, J. S.; Seeger, R. *Int. J. Quantum Chem., Symp.* **1976**, *10*, 1.
(52) Frisch, M. J.; Head-Gordon, M.; Pople, J. A. *Chem. Phys. Lett.* **1990**, *166*, 275.
(53) Fletcher, G. D.; Schmidt, M. W.; Gordon, M. S. *Adv. Chem. Phys.* **1999**, *110*, 267.
(54) Aikens, C. M.; Webb, S. P.; Bell, R. L.; Fletcher, G. D.; Schmidt, M. W.; Gordon, M. S. *Theor. Chem. Acc.* **2003**, *110*, 233.
(55) Merrill, G. N.; Webb, S. P.; Bivin, D. B. *J. Phys. Chem. A* **2003**, *107*, 386.
(56) Webb, S. P.; Gordon, M. S. *J. Phys. Chem. A* **1999**, *103*, 1265.
(57) Adamovic, I.; Gordon, M. S. *J. Phys. Chem. A* **2005**, *109*, 1629.
(58) Day, P. N.; Pachter, R.; Gordon, M. S.; Merrill, G. N. *J. Chem. Phys.* **2000**, *112*, 2063.
(59) Hehre, W. J.; Ditchfield, R.; Pople, J. A. *J. Chem. Phys.* **1972**, *56*, 2257.
(60) Francl, M. M.; Pietro, W. J.; Hehre, W. J.; Binkley, J. S.; Gordon, M. S.; DeFrees, D. J.; Pople, J. A. *J. Chem. Phys.* **1982**, *77*, 3654.
(61) Hariharan, P. C.; Pople, J. A. *Theor. Chim. Acta* **1973**, *28*, 213.
(62) Clark, T.; Chandrasekhar, J.; Schleyer, P. v. R. *J. Comput. Chem.* **1983**, *4*, 294.
(63) Schmidt, M. W.; Baldridge, K. K.; Boatz, J. A.; Jensen, J. H.; Koseki, S.; Matsunaga, N.; Gordon, M. S.; Ngugen, K. A.; Su, S.; Windus, T. L.; Elbert, S. T.; Montgomery, J.; Dupuis, M. *J. Comput. Chem.* **1993**, *14*, 1347.
(64) Metropolis, N.; Rosenbluth, A.; Tellor, A. *J. Chem. Phys.* **1953**, *21*, 1089.
(65) Kirkpatrick, S.; Gelatt, C. D.; Vecchi, M. P. *Science* **1983**, *220*, 671.
(66) Krishnan, R.; Binkley, J. S.; Pople, J. A. *J. Chem. Phys.* **1980**, *72*, 650.
(67) Frisch, M. J.; Pople, J. A.; Binkley, J. S. *J. Chem. Phys.* **1984**, *80*, 3265.
(68) Crawford, T. D.; Schaefer, H. F.; Lipkowitz, K. B.; Boyd, D. B. *Rev. Comput. Chem.* **2000**, *14*, 33.
(69) Piecuch, P.; Kucharski, S. A.; Kowalski, K.; Musial, M. *Comput. Phys. Commun.* **2002**, *149*, 71.
(70) Hiraoka, K.; Mizuse, S.; Yamabe, S. *J. Phys. Chem.* **1988**, *92*, 3943.
(71) Arshadi, M.; Yamdagni, R.; Kebarle, P. *J. Phys. Chem.* **1970**, *74*, 1475.